Observation of Hard Processes in Rapidity Gap Events in γp Interactions at HERA

H1 Collaboration

Abstract:

Events with no hadronic energy flow in a large interval of pseudo-rapidity in the proton direction are observed in photon-proton interactions at an average centre of mass energy $< \sqrt{s_{\gamma p}} >$ of 200 GeV. These events are interpreted as photon diffractive dissociation. Evidence for hard scattering in photon diffractive dissociation is demonstrated using inclusive single particle spectra, thrust as a function of transverse energy, and the observation of jet production. The data can be described by a Monte Carlo calculation including hard photon-Pomeron scattering.

H1 Collaboration

T. Ahmed[3], S. Aid[13], V. Andreev[24], B. Andrieu[28], R.-D. Appuhn[11], M. Arpagaus[36], A. Babaev[26], J. Baehr[35], J. Bán[17], P. Baranov[24], E. Barrelet[29], W. Bartel[11], M. Barth[4], U. Bassler[29], H.P. Beck[37], H.-J. Behrend[11], A. Belousov[24], Ch. Berger[1], H. Bergstein[1], G. Bernardi[29], R. Bernet[36], G. Bertrand-Coremans[4], M. Besançon[9], R. Beyer[11], P. Biddulph[22], J.C. Bizot[27], V. Blobel[13], K. Borras[8], F. Botterweck[4], V. Boudry[28], A. Braemer[14], F. Brasse[11], W. Braunschweig[1], V. Brisson[27], D. Bruncko[17], C. Brune[15], R.Buchholz[11], L. Büngener[13], J. Bürger[11], F.W. Büsser[13], A. Buniatian[11,39], S. Burke[18], G. Buschhorn[26], A.J. Campbell[11], T. Carli[26], F. Charles[11], D. Clarke[5], A.B. Clegg[18], B. Clerbaux[4], M. Colombo[8], J.G. Contreras[8], J.A. Coughlan[5], A. Courau[27], Ch. Coutures[9], G. Cozzika[9], L. Criegee[11], D.G. Cussans[5], J. Cvach[30], S. Dagoret[29], J.B. Dainton[19], M. Danilov[23], W.D. Dau[16], K. Daum[34], M. David[9], E. Deffur[11], B. Delcourt[27], L. Del Buono[29], A. De Roeck[11], E.A. De Wolf[4], P. Di Nezza[32], C. Dollfus[37], J.D. Dowell[3], H.B. Dreis[2], V. Droutskoi[23], J. Duboc[29], D. Düllmann[13], O. Dünger[13], H. Duhm[12], J. Ebert[34], T.R. Ebert[19], G. Eckerlin[11], V. Efremenko[23], S. Egli[37], H. Ehrlichmann[35], S. Eichenberger[37], R. Eichler[36], F. Eisele[14], E. Eisenhandler[20], R.J. Ellison[22], E. Elsen[11], M. Erdmann[14], W. Erdmann[36], E. Evrard[4], L. Favart[4], A. Fedotov[23], D. Feeken[13], R. Felst[11], J. Feltesse[9], J. Ferencei[15], F. Ferrarotto[32], K. Flamm[11], M. Fleischer[11], M. Flieser[26], G. Flügge[2], A. Fomenko[24], B. Fominykh[23], M. Forbush[7], J. Formánek[31], J.M. Foster[22], G. Franke[11], E. Fretwurst[12], E. Gabathuler[19], K. Gabathuler[33], K. Gamerdinger[26], J. Garvey[3], J. Gayler[11], M. Gebauer[8], A. Gellrich[11], H. Genzel[1], R. Gerhards[11], U. Goerlach[11], L. Goerlich[6], N. Gogitidze[24], M. Goldberg[29], D. Goldner[8], B. Gonzalez-Pineiro[29], A.M. Goodall[19], I. Gorelov[23], P. Goritchev[23], C. Grab[36], H. Grässler[2], R. Grässler[2], T. Greenshaw[19], G. Grindhammer[26], A. Gruber[26], C. Gruber[16], J. Haack[35], D. Haidt[11], L. Hajduk[6], O. Hamon[29], M. Hampel[1], E.M. Hanlon[18], M. Hapke[11], W.J. Haynes[5], J. Heatherington[20], G. Heinzelmann[13], R.C.W. Henderson[18], H. Henschel[35], R. Herma[1], I. Herynek[30], M.F. Hess[26], W. Hildesheim[12], P. Hill[5], K.H. Hiller[35], C.D. Hilton[22], J. Hladký[30], K.C. Hoeger[22], M. Höppner[8], R. Horisberger[33], Ph. Huet[4], H. Hufnagel[14], M. Ibbotson[22], H. Itterbeck[1], M.-A. Jabiol[9], A. Jacholkowska[27], C. Jacobsson[21], M. Jaffre[27], J. Janoth[15], T. Jansen[11], L. Jönsson[21], K. Johannsen[13], D.P. Johnson[4], L. Johnson[18], H. Jung[29], P.I.P. Kalmus[20], D. Kant[20], R. Kaschowitz[2], P. Kasselmann[12], U. Kathage[16], H.H. Kaufmann[35], S. Kazarian[11], I.R. Kenyon[3], S. Kermiche[25], C. Keuker[1], C. Kiesling[26], M. Klein[35], C. Kleinwort[13], G. Knies[11], W. Ko[7], T. Köhler[1], H. Kolanoski[8], F. Kole[7], S.D. Kolya[22], V. Korbel[11], M. Korn[8], P. Kostka[35], S.K. Kotelnikov[24], T. Krämerkämper[8], M.W. Krasny[6,29], H. Krehbiel[11], D. Krücker[2], U. Krüger[11], U. Krüner-Marquis[11], J.P. Kubenka[26], H. Küster[2], M. Kuhlen[26], T. Kurča[17], J. Kurzhöfer[8], B. Kuznik[34], D. Lacour[29], F. Lamarche[28], R. Lander[7], M.P.J. Landon[20], W. Lange[35], P. Lanius[26], J.-F. Laporte[9], A. Lebedev[24], C. Leverenz[11], S. Levonian[11,24], Ch. Ley[2], A. Lindner[8], G. Lindström[12], F. Linsel[11], J. Lipinski[13], B. List[11], P. Loch[27], H. Lohmander[21], G.C. Lopez[20], V. Lubimov[23], D. Lüke[8,11], N. Magnussen[34], E. Malinovski[24], S. Mani[7], R. Maraček[17], P. Marage[4], J. Marks[25], R. Marshall[22], J. Martens[34], R. Martin[11], H.-U. Martyn[1], J. Martyniak[6], S. Masson[2], T. Mavroidis[20], S.J. Maxfield[19], S.J. McMahon[19], A. Mehta[22], K. Meier[15], D. Mercer[22], T. Merz[11], C.A. Meyer[37], H. Meyer[34], J. Meyer[11], S. Mikocki[6], D. Milstead[19], F. Moreau[28], J.V. Morris[5], G. Müller[11], K. Müller[37], P. Murín[17], V. Nagovizin[23], R. Nahnhauer[35], B. Naroska[13], Th. Naumann[35], P.R. Newman[3], D. Newton[18], D. Neyret[29], H.K. Nguyen[29], F. Niebergall[13], C. Niebuhr[11], R. Nisius[1], G. Nowak[6], G.W. Noyes[5], M. Nyberg-Werther[21], H. Oberlack[26], U. Obrock[8], J.E. Olsson[11], E. Panaro[12], A. Panitch[4], C. Pascaud[27], G.D. Patel[19], E. Peppel[35], E. Perez[9], J.P. Phillips[22], Ch. Pichler[12], D. Pitzl[36], G. Pope[7], S. Prell[11], R. Prosi[11], G. Rädel[11], F. Raupach[1], P. Reimer[30], S. Reinshagen[11], P. Ribarics[26], H.Rick[8], V. Riech[12], J. Riedlberger[36], S. Riess[13], M. Rietz[2], S.M. Robertson[3], P. Robmann[37], H.E. Roloff[35], R. Roosen[4], K. Rosenbauer[1] A. Rostovtsev[23], F. Rouse[7], C. Royon[9], K. Rüter[26], S. Rusakov[24], K. Rybicki[6], R. Rylko[20], N. Sahlmann[2], E. Sanchez[26], D.P.C. Sankey[5],

M. Savitsky[23], P. Schacht[26], S. Schiek[11], P. Schleper[14], W. von Schlippe[20], C. Schmidt[11], D. Schmidt[34], G. Schmidt[13], A. Schöning[11], V. Schröder[11], E. Schuhmann[26], B. Schwab[14], A. Schwind[35], U. Seehausen[13], F. Sefkow[11], M. Seidel[12], R. Sell[11], A. Semenov[23], V. Shekelyan[23], I. Sheviakov[24], H. Shooshtari[26], L.N. Shtarkov[24], G. Siegmon[16], U. Siewert[16], Y. Sirois[28], I.O. Skillicorn[10], P. Smirnov[24], J.R. Smith[7], Y. Soloviev[24], H. Spitzer[13], R. Starosta[1], M. Steenbock[13], P. Steffen[11], R. Steinberg[2], B. Stella[32], K. Stephens[22], J. Stier[11], J. Stiewe[15], U. Stösslein[35], J. Strachota[30], U. Straumann[37], W. Struczinski[2], J.P. Sutton[3], S. Tapprogge[15], R.E. Taylor[38,27], V. Tchernyshov[23], C. Thiebaux[28], G. Thompson[20], P. Truöl[37], J. Turnau[6], J. Tutas[14], P. Uelkes[2], A. Usik[24], S. Valkár[31], A. Valkárová[31], C. Vallée[25], P. Van Esch[4], P. Van Mechelen[4], A. Vartapetian[11,39], Y. Vazdik[24], M. Vecko[30], P. Verrecchia[9], G. Villet[9], K. Wacker[8], A. Wagener[2], M. Wagener[33], I.W. Walker[18], A. Walther[8], G. Weber[13], M. Weber[11], D. Wegener[8], A. Wegner[11], H.P. Wellisch[26], L.R. West[3], S. Willard[7], M. Winde[35], G.-G. Winter[11], A.E. Wright[22], E. Wünsch[11], N. Wulff[11], T.P. Yiou[29], J. Žáček[31], D. Zarbock[12], Z. Zhang[27], A. Zhokin[23], M. Zimmer[11], W. Zimmermann[11], F. Zomer[27] and K. Zuber[15]

[1] *I. Physikalisches Institut der RWTH, Aachen, Germany*[a]
[2] *III. Physikalisches Institut der RWTH, Aachen, Germany*[a]
[3] *School of Physics and Space Research, University of Birmingham, Birmingham, UK*[b]
[4] *Inter-University Institute for High Energies ULB-VUB, Brussels; Universitaire Instellingen Antwerpen, Wilrijk, Belgium*[c]
[5] *Rutherford Appleton Laboratory, Chilton, Didcot, UK*[b]
[6] *Institute for Nuclear Physics, Cracow, Poland*[d]
[7] *Physics Department and IIRPA, University of California, Davis, California, USA*[e]
[8] *Institut für Physik, Universität Dortmund, Dortmund, Germany*[a]
[9] *CEA, DSM/DAPNIA, CE-SACLAY, Gif-sur-Yvette, France*
[10] *Department of Physics and Astronomy, University of Glasgow, Glasgow, UK*[b]
[11] *DESY, Hamburg, Germany*[a]
[12] *I. Institut für Experimentalphysik, Universität Hamburg, Hamburg, Germany*[a]
[13] *II. Institut für Experimentalphysik, Universität Hamburg, Hamburg, Germany*[a]
[14] *Physikalisches Institut, Universität Heidelberg, Heidelberg, Germany*[a]
[15] *Institut für Hochenergiephysik, Universität Heidelberg, Heidelberg, Germany*[a]
[16] *Institut für Reine und Angewandte Kernphysik, Universität Kiel, Kiel, Germany*[a]
[17] *Institute of Experimental Physics, Slovak Academy of Sciences, Košice, Slovak Republic*
[18] *School of Physics and Materials, University of Lancaster, Lancaster, UK*[b]
[19] *Department of Physics, University of Liverpool, Liverpool, UK*[b]
[20] *Queen Mary and Westfield College, London, UK*[b]
[21] *Physics Department, University of Lund, Lund, Sweden*[f]
[22] *Physics Department, University of Manchester, Manchester, UK*[b]
[23] *Institute for Theoretical and Experimental Physics, Moscow, Russia*
[24] *Lebedev Physical Institute, Moscow, Russia*
[25] *CPPM, Université d'Aix-Marseille II, IN2P3-CNRS, Marseille, France*
[26] *Max-Planck-Institut für Physik, München, Germany*[a]
[27] *LAL, Université de Paris-Sud, IN2P3-CNRS, Orsay, France*
[28] *LPNHE, Ecole Polytechnique, IN2P3-CNRS, Palaiseau, France*
[29] *LPNHE, Universités Paris VI and VII, IN2P3-CNRS, Paris, France*
[30] *Institute of Physics, Czech Academy of Sciences, Praha, Czech Republic*[g]
[31] *Nuclear Center, Charles University, Praha, Czech Republic*[g]
[32] *INFN Roma and Dipartimento di Fisica, Universita "La Sapienza", Roma, Italy*
[33] *Paul Scherrer Institut, Villigen, Switzerland*
[34] *Fachbereich Physik, Bergische Universität Gesamthochschule Wuppertal, Wuppertal, Germany*[a]
[35] *DESY, Institut für Hochenergiephysik, Zeuthen, Germany*[a]

[36] *Institut für Teilchenphysik, ETH, Zürich, Switzerland*[h]
[37] *Physik-Institut der Universität Zürich, Zürich, Switzerland*[h]
[38] *Stanford Linear Accelerator Center, Stanford California, USA*
[39] *Visitor from Yerevan Phys.Inst., Armenia*

[a] *Supported by the Bundesministerium für Forschung und Technologie, FRG under contract numbers 6AC17P, 6AC47P, 6DO57I, 6HH17P, 6HH27I, 6HD17I, 6HD27I, 6KI17P, 6MP17I, and 6WT87P*
[b] *Supported by the UK Particle Physics and Astronomy Research Council, and formerly by the UK Science and Engineering Research Council*
[c] *Supported by FNRS-NFWO, IISN-IIKW*
[d] *Supported by the Polish State Committee for Scientific Research, grant No. 204209101*
[e] *Supported in part by USDOE grant DE F603 91ER40674*
[f] *Supported by the Swedish Natural Science Research Council*
[g] *Supported by GA ČR, grant no. 202/93/2423 and by GA AV ČR, grant no. 19095*
[h] *Supported by the Swiss National Science Foundation*

1 Introduction

The electron-proton collider HERA has turned out to be an important research facility for the understanding of high energy photon-hadron interactions [1-7]. Quasi-real photons are produced in ep collisions by electrons which are scattered through small angles. Photon-proton centre of mass system (CMS) energies of up to 300 GeV are possible. This is one order of magnitude larger than the CMS energies achieved so far in fixed target experiments. At these energies high mass diffractive dissociation processes in photoproduction can be studied.

The hadronic interaction of quasi-real photons with matter is fairly well described by a model where the photon converts into a virtual hadronic state, mainly the $\rho^0(770)$ meson, and subsequently interacts with a target hadron. In recent γp studies it was shown that, similar to hadron-hadron scattering, photoproduction exhibits both the production of transverse jets and a substantial rate of events which contain particles with transverse momenta p_T values larger than a few GeV [1-6]. These phenomena can be readily interpreted in terms of the interaction of a parton in the incident hadron and a parton in the photon, and is termed a *resolved photon* process. In addition to the resolved process the photon can couple directly to quarks in the proton. This is termed a *direct photon* process. Models including leading order (LO) QCD diagrams for resolved and direct processes indeed describe the gross features of these data.

As a result of the similarity with hadron-hadron collisions, one expects a diffractive scattering component in the γp cross section. Diffractive scattering involves the exchange of energy-momentum between the incident hadrons, but no exchange of quantum numbers. The diffractive cross section is expected to be large, namely about 30% of the total cross section.

In diffractive processes both incident particles can keep their original identity (elastic scattering), or one or both of them can dissociate i.e. break up into a system of generally low invariant mass and low multiplicity (diffractive dissociation). For single diffractive dissociation only one of the incident particles dissociates after the interaction, while for double diffractive dissociation both incident particles dissociate. At HERA it is possible to study the single diffractive dissociation channels $Vp \to Xp$ (meson diffractive dissociation) and $Vp \to VX$ (proton diffractive dissociation), where V stands for a vector meson ($\rho^0(770)$, $\omega(782)$, $\phi(1020)$, etc.). A salient feature of single diffractive dissociation at high centre of mass energies is a gap in rapidity between the non-dissociated hadron and the particles of the dissociated system. Due to the asymmetry between the incident proton (820 GeV) and electron (26.7 GeV) energies, we can identify meson diffractive interactions by requiring the absence of energy in the region of the HERA detectors around the proton direction. The diffractive interaction events, which will be isolated by the rapidity gap cut detailed below, are the sum of meson single diffractive dissociation and a contamination of double diffractive dissociation, and are termed *photon diffractive dissociation* in the following. The contamination of elastic events $Vp \to Vp$ and proton single diffractive dissociation events $Vp \to VX$ seen in the detector is negligible ($< 1\%$), as well as that of events resulting from other Reggeon exchanges.

Phenomenologically, the observed properties of the diffractive cross section are described by triple-Regge theory where this process is viewed as the exchange of a Pomeron [8]. This interpretation however gives no information on the details of the hadronic final states produced in diffractive dissociation. Traditionally the final state in diffractive dissociation is assumed to be described by a multiperipheral [9] type of model in which particles are distributed throughout the final state phase space with limited transverse momentum. This approach has been used successfully so far for comparisons with the available measurements of multiplicity and rapidity distributions of charged particles from the diffractive system. On the other hand, in modern QCD language it is tempting to consider the Pomeron as a partonic system [10] which can be probed in a hard scattering process. Models based on this idea assume that the Pomeron behaves as a hadron and the concept of a Pomeron structure function is introduced [11-13]. In contrast to the

approach of assuming limited p_T phase space, these models predict that, similar to high energy hadron-hadron scattering, high mass diffractive dissociation exhibits the production of jets and a large p_T tail in the differential transverse momentum distribution. Thus hard hadron-Pomeron scattering events should be observed in diffractive hadronic collisions at high energies. The UA8 collaboration recently has shown evidence for jet production in diffractive $p\overline{p}$ events [14], interpreted as resulting from the collisions of partons from the proton with partons from the Pomeron. Furthermore, within this partonic picture, these data have shown sensitivity to the parton distribution in the Pomeron. New data to study the partonic structure of the Pomeron are essential to check this picture. In particular the p_T spectra of particles, the transverse thrust distribution, and the jet production spectra are expected to provide important information on the underlying dynamics of the diffractive process.

This analysis presents the study of events with a rapidity gap in photoproduction at HERA. Based on the comparison with Monte Carlo calculations these events are found to be well compatible with the hypothesis of photon diffractive dissociation. Evidence for hard scattering properties of these events is presented. The present analysis is based on data collected in 1993 with the H1 detector at HERA, for collisions of e and p beams with energies of 26.7 GeV and 820 GeV respectively.

2 Experimental Set-up

The H1 detector is described in detail elsewhere [15]. Here we describe briefly the components of the detector relevant for this analysis.

Measurements of charged particle tracks and the interaction vertex are provided by a central and forward tracking system, consisting of drift and multiwire proportional chambers. The central and forward tracking chambers cover the complete azimuth and the range from about -2.0 to 3.0 in pseudo-rapidity $\eta = -\ln(\tan(\theta/2))$. Here θ is a polar angle with respect to the proton beam direction (z axis), termed the forward region. Tracks found in the central and forward tracker are used to define the event vertex of the interaction. In this analysis we use for the inclusive single particle analysis tracks fitted to the event vertex, with a minimum p_T of 150 MeV/c and $\mid z_{TRACK} - z_{VERTEX} \mid < 12$ cm, with z_{TRACK} being the z-value of the track at the distance of closest approach. The central chamber is interspersed by an inner and an outer double layer of cylindrical multiwire proportional chambers (MWPC). Together with MWPCs from the forward tracking system, these chambers were used in the trigger to select events with charged tracks pointing to the interaction region. The MWPC trigger covers the rapidity range from -1.5 to 2.8.

The tracking region is surrounded by a fine grained liquid argon (LAr) calorimeter [16] consisting of an electromagnetic section with lead absorber and a hadronic section with steel absorber. The energy resolutions achieved in test beams were $\sigma/E \approx 12\%/\sqrt{E}$ for electrons and $\approx 50\%/\sqrt{E}$ for pions, with E in GeV [15, 17]. The LAr calorimeter covers the complete azimuth and the range from -1.5 to 3.65 in pseudo-rapidity η. The backward region ($-3.3 < \eta < -1.5$) is covered by a lead-scintillator electromagnetic calorimeter (BEMC). For the measurement of the energy flow we use the cells of the LAr calorimeter and of the BEMC. The reconstruction of calorimetric energies is described in more detail in [15, 17]. For the transverse thrust analysis tracks are also included. The calorimeters and the tracking system are placed inside a superconducting solenoid which, together with the surrounding octagonal iron yoke, maintains a uniform magnetic field of 1.15 T along z in the tracking region.

An electron detector placed at a distance of $z = -33$ m allows tagging of electrons scattered at small angles $\theta' < 5$ mrad ($\theta' = \pi - \theta$) from photoproduction processes. Together with a photon

detector at $z = -103$ m the electron tagger is used to measure Bethe-Heitler $ep \to ep\gamma$ events for luminosity determination. Both detectors are TlCl/TlBr crystal Čerenkov calorimeters with an energy resolution of $10\%/\sqrt{E}$.

3 Event Selection

This analysis is based on a sample of tagged events in which the energy of the scattered electron is measured in the H1 small angle electron tagger. This limits the acceptance for the virtuality of the incident photons to the range 3×10^{-8} GeV^2 $< Q^2 < 10^{-2}$ GeV^2 where Q^2 is given by $Q^2 = 4E_e E'_e \cos^2(\theta_e/2)$. Here E_e and E'_e are the energies of the incoming and scattered electron respectively and θ_e is the angle of the scattered electron with respect to the proton direction. The fractional energy of the photon as measured by the small angle electron detector is required to be in the interval $0.25 < y < 0.7$, where $y = 1 - E'_e/E_e$. This range in y corresponds to the energy interval of the γp system (W) from 150 GeV to 250 GeV, with an average of about 200 GeV. The condition on y removes events from the tails of the electron energy distribution where the acceptance of the electron tagger is small. It also removes the elastic $Vp \to Vp$ and single proton diffraction dissociation $Vp \to VX$ component where, due to the event kinematics, the vector meson escapes detection.

We use two data samples in this analysis. A first data sample, henceforth called *minimum bias sample*, has been collected with a loose, minimum bias trigger, designed for collecting events for general multiparticle studies of γp collisions. This trigger was only active for an equivalent integrated luminosity of 117 nb^{-1}. A second data sample, henceforth called *jet sample*, was collected with a more selective trigger but permits the use of a data sample corresponding to an integrated luminosity of 289 nb^{-1}.

A coincidence of the small angle electron detector signal ($E'_e > 4$ GeV) with at least one track pointing to the vertex region was used to trigger on events from interactions of protons with quasi-real photons. For the minimum bias sample, the track condition is derived from a very rough measurement from the MWPC trigger and requires a track $p_T \gtrsim 150$ MeV/c. The acceptance of this trigger was studied in [7]. For the jet sample, a more restrictive track trigger condition was used which was based on fast signals of the central drift chamber trigger. It required a well defined track with $p_T \gtrsim 450$ MeV/c in a polar angular interval of $25^0 < \theta < 155^0$.

The events kept by these trigger conditions were reconstructed and subjected to the following selection criteria. Events were accepted if, apart from the electron tagger energy conditions given above, at least one track originated from the interaction region in the transverse (x, y) plane, and thus an interaction vertex was reconstructed. This event vertex must lie in z within the region ($-35 < z < 25$ cm), the length of which is governed by the total proton bunch length. In addition, for the jet sample we required the events to contain a minimum transverse energy, E_T, of 5 GeV. With this requirement the trigger used for this sample was found to have an unbiased acceptance for events with jets. Throughout this paper the transverse energy is defined with respect to the γp axis.

Events containing cosmic ray showers and beam halo muons were rejected by means of patterns recognized in the central tracking system and in the LAr calorimeter. Interactions of the proton beam with the residual gas in the fiducial vertex region in random coincidence with a signal in the electron tagger are removed by appropriate cuts on low y_h in coincidence with large $\sum p_z / \sum p$ values (see [7] for details). Here $y_h = \sum(E - p_z)/(2 \cdot E_e)$ is measured in the calorimeter where $\sum(E - p_z)$ is determined by summing $E \cdot (1 - \cos\theta)$ for all cells, and p_z denotes the longitudinal momentum component.

In total about 125,000 events satisfy the final selection criteria for the minimum bias sample and 174,000 events for the jet sample.

In the following the uncorrected data will be compared with Monte Carlo predictions which were simulated through the detector and reconstructed as for the real data. The detailed simulation of the detector parts is described in [15]. All figures are shown with statistical errors only. The QED radiative corrections to the jet cross section are expected to be small ($\lesssim 2\%$) for the present experimental conditions and have not been considered in this analysis.

4 Monte Carlo Simulation Programs

Soft hadronic events, i.e. events with no hard scale, are generated with the PYTHIA5.6 [18] Monte Carlo program which includes the diffractive components of the γp cross section. The differential cross section for diffractive events follows the properties known from hadronic diffractive dissociation, namely an exponential t dependence and a $1/M_X^2$ behaviour. Here t is the four momentum transfer between the incident particles and M_X is the invariant mass of the diffractive system. Experimentally this behaviour in M_X^2 and t has been confirmed in a fixed target photoproduction experiment [19]. The diffractive system fragments into hadrons and produces a final state involving essentially only fragmentation p_T for the produced hadrons. This model reproduces the kinematic properties of a longitudinal phase space model. Henceforth it is referred to as the *soft diffractive model*.

For further study we use a model which explicitely includes *diffractive hard scattering*: POMPYT1.0 [20]. This model assumes the emission of a (space-like) Pomeron at the proton vertex. The resulting photon-Pomeron interaction is simulated as the hard scattering of the photon (direct process) or partons in the photon (resolved process) with partons in the Pomeron according to LO QCD calculations for the hard scattering processes. These collisions give rise to the production both of particles with a large p_T and of jets.

To compare with non-diffractive hard scattering in photon-hadron interactions, the Monte Carlo program PYTHIA5.6 was used in its high p_T option for photoproduction. Here γp interactions are simulated as the hard scattering of the partons in the photon and in the proton, according to the LO QCD calculations, summing the contributions from direct and resolved photon interactions. The effects of initial and final state QCD radiation are described by leading logarithm type parton showers. The possibility of multiple interactions between the partons from the photon and proton is included. This model is referred to as the *non-diffractive model* in the following. It describes well the basic features of the high p_T inclusive γp data [3].

Both the high p_T PYTHIA and POMPYT models are based on LO QCD calculations. Since a QCD calculation is divergent for $\hat{p}_T \to 0$, where $\hat{p}_T$ is the transverse momentum of the outgoing partons in the hard scattering process, a minimum $\hat{p}_T$ cut-off value $\hat{p}_T^{min}$ is applied. For this analysis the cut-off has been chosen to be $\hat{p}_T^{min} = 2.0$ GeV/c. Due to the divergence, no absolute normalization of the Monte Carlo predictions will be used in the following. Instead comparisons are made with the Monte Carlo calculations normalized to the number of events in the data in the regions where these models are expected to be applicable. For the parton distributions we use GRV leading order parametrizations both for the proton [21] and the photon [22]. In this analysis the Pomeron was assumed to consist of gluons and their distribution function within the Pomeron was taken to be either "hard", $zg(z) \sim z(1-z)$, hereafter labelled "$G0$", or "soft", $zg(z) \sim (1-z)^5$, hereafter labelled "$G5$". The variable $z = x_{g/I\!P}$ is the fraction of the Pomeron momentum carried by the struck gluon involved in the interaction. The results from high p_T jet production in diffractive proton anti-proton interactions mentioned above favour the hard $G0$ distribution. Unless otherwhise specified we use for comparison with the data the $G0$ densities for the Pomeron. For hadronic fragmentation the Lund model [23] is used in all Monte Carlo programs.

5 Rapidity Gap Events

The energy flow for the selected events was investigated using the variable η_{max}, the pseudo-rapidity either of the most forward calorimetric energy deposit of 400 MeV or the most forward detected track with a transverse momentum $p_T > 150$ MeV/c. In fig. 1 the η_{max} spectrum is shown for the minimum bias sample of photoproduction events. The largest pseudo-rapidity which can be observed in the H1 liquid argon calorimeter, η_{Lar}, is about 3.65 and in the forward tracker, η_{FT}, about 3. These values vary slightly due to the position of the ep event vertex. Fig. 1 shows that for most events there is energy close to η_{Lar}. However there is also a class of events which have a small η_{max} value, i.e. a large empty region in the calorimeter in the proton direction.

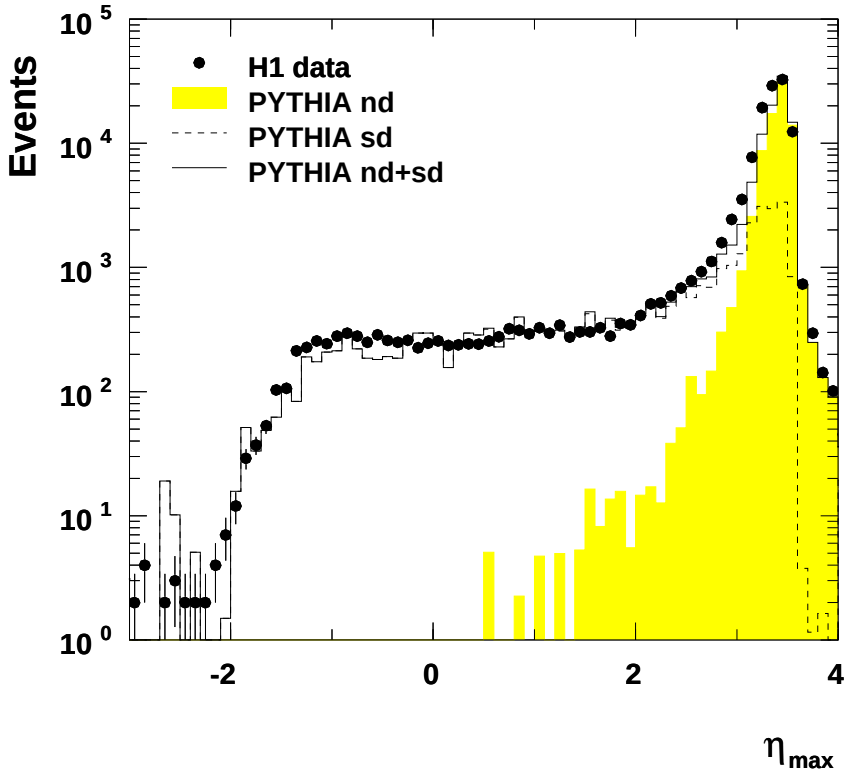

Figure 1: Maximum peudo-rapidity η_{max} distribution in γp events compared to a diffractive (dashed line) and a non-diffractive (shaded area) Monte Carlo model, and their sum (full line).

The η_{max} spectrum can be qualitatively understood by comparing it with model predictions for diffractive and non-diffractive processes. The comparison with the PYTHIA Monte Carlo predictions in fig. 1 shows that the events with small η_{max} are consistent with photon diffractive dissociation. The non-diffractive prediction (PYTHIA-nd; shaded area) exhibits a sharp fall off with increasing gap size, i.e. decreasing η_{max}, and clearly does not account for the η_{max} tail for $\eta_{max} < 2$. The photon diffractive dissociation component (PYTHIA-sd ; dashed line), calculated with the soft diffractive model, gives a good description of the spectrum for $\eta_{max} < 2$. The shape of the η_{max} distribution for the Monte Carlo events with a rapidity gap results from the $1/M_X^2$ ansatz for the differential diffractive cross section. The distribution for the soft diffractive model is normalised to the region $\eta_{max} < 2$, while the distribution for the non-diffractive model is normalised to $\eta_{max} > 3$. In all, the sum of the soft diffractive and non-diffractive γp Monte Carlo calculations (full line) accounts reasonably well for the observed η_{max} spectrum. This observation does not change by varying the minimum cluster energy and the track p_T requirements by 30%.

Other production mechanisms for producing rapidity gap events can be envisaged. Other Reggeon exchanges (e.g. π, $f_2(1270)$... exchange) can give rise to rapidity gaps as well. However

due to the nature of the η_{max} cut applied here, we implicitely select a region of $M_x^2/s \approx x_{I\!P/p} < 10^{-2}$, where Pomeron exchange is expected to dominate over Reggeon exchange [24]. Here $x_{I\!P/p}$ is the momentum fraction of the proton carried by the Pomeron.

To study the properties of the rapidity gap events, we select events with $\eta_{max} < 1.5$. We additionally require for this and all further analyses in this paper that the calorimetric energy with $\eta > 1.5$ be less than 1 GeV and that the forward rapidity gap be the largest in the event. These additional requirements remove only a few % of the events with a forward rapidity gap, but enhance the purity of the sample. In total 7249 events survive this cut for the minimum bias sample. A consequence of this η_{max} selection is that diffractive events with a dissociative system of mass M_X less than about 20 GeV are selected. The background in the rapidity gap data sample, due to accidental coincidence of a proton beam gas interaction with an electron scattered at small angle in the same event, was estimated to be 4 events using data taken with a non-colliding proton bunch (pilot bunches) and using the rate of the small angle electron detector alone. This background is neglected in the following. The remaining background from electron gas events was found to be more important. From electron pilot bunch studies we derived a contamination of 6% in the minimum bias sample. This background is subtracted statistically from the data presented in this section.

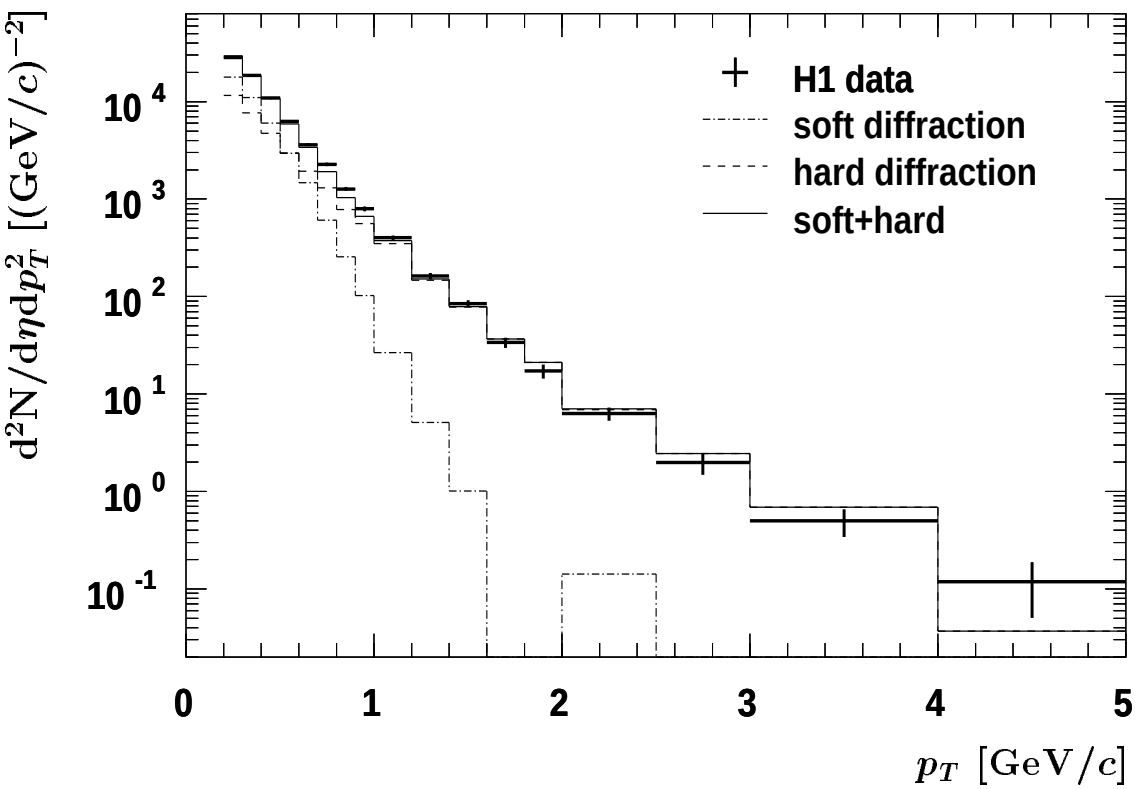

Figure 2: Transverse momentum distribution of charged particles for events with large pseudo-rapidity gap (η_{max} <1.5) compared to Monte Carlo predictions, explained in the text.

If diffractive dissociation involves a hard process then the corresponding underlying parton interaction should be detectable in the event shape at the hadronic level. Possible signatures should be a large p_T tail in the inclusive single particle distribution, and an azimuthal back to back correlation of transverse energy flow, growing with E_T of the event. Such a correlation can be quantified by studying the thrust in the transverse momentum plane.

In figure 2 the p_T spectrum for charged tracks in the range $-1.5 < \eta < 1.5$ is shown, where p_T is measured with respect to the beam axis. The shape of the distribution shows an exponential fall off at small p_T values with a large tail extending to $p_T \sim 5$ GeV/c. The same observation

was made for the p_T spectrum measured in the total inclusive photoproduction sample [3], where the events in the tail were identified with hard scattering in γp interactions. The shape of the p_T spectrum is compared with the soft diffractive model prediction from PYTHIA (dashed-dotted line) and the diffractive hard scattering model prediction from POMPYT (dashed line). For purpose of display the POMPYT prediction is normalised to the region $p_T > 1.5$ GeV/c, and the sum of POMPYT and PYTHIA is normalised to the total spectrum. The soft diffractive model describes well the exponential fall of the data at small p_T which represents the bulk of the data, but clearly cannot account for the p_T tail. POMPYT gives a satisfactory description of the large p_T region. The overall p_T distribution is well described by the sum of a soft and hard diffractive component (full line). Events from hard scattering of the partonic content of the photon with the proton, i.e. the remaining non-diffractive events in the rapidity gap sample, are predicted to give a small contribution to the p_T spectrum, namely less than 20 events. Similar results were obtained from studies of the transverse energy spectrum of the rapidity gap events (not shown). The agreement with the diffractive hard scattering model may thus be taken as an indication for hard scattering at the parton level in photon diffraction.

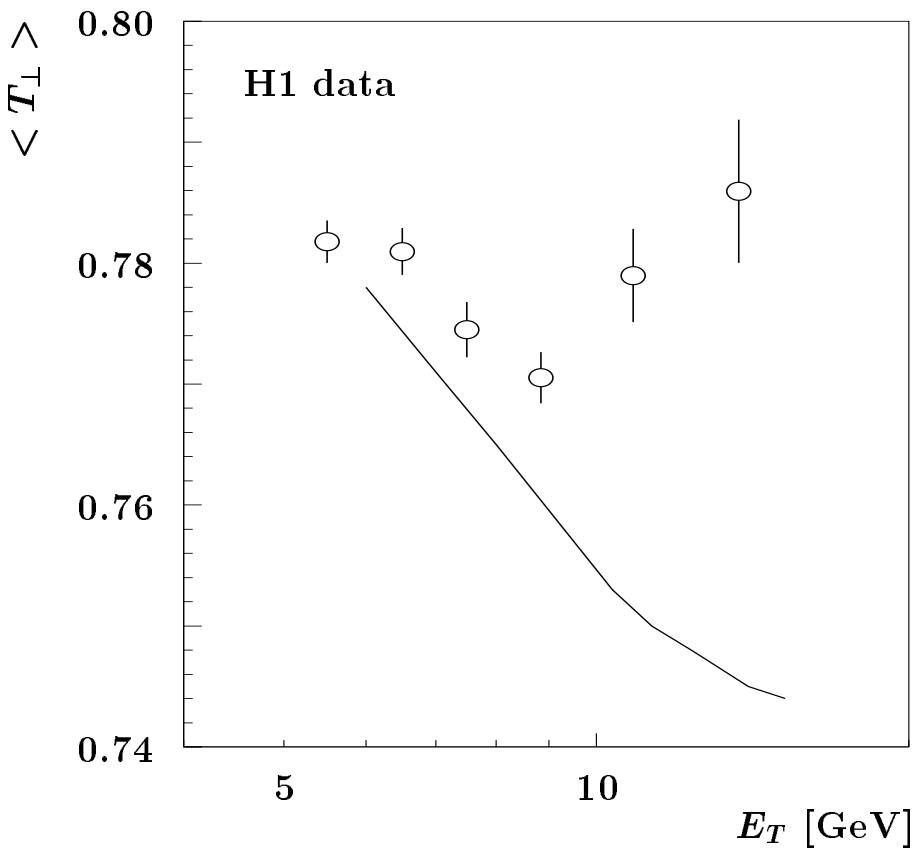

Figure 3: Average observed transverse thrust as function of event E_T. Data (points) and expectation for azimuthally isotropic events (line) with the same average multiplicity as the data points for a given E_T.

A variable sensitive to the event shape is the transverse thrust $T_\perp = \max(\sum \mathbf{p_T} \cdot \mathbf{n} / \sum |\mathbf{p_T}|)$ calculated from charged tracks and calorimetric clusters, without double counting. Here $\mathbf{p_T}$ is the transverse momentum vector for each final state object, and $|\mathbf{n}| = 1$. The transverse thrust axis is given by the $\mathbf{n}$ vector for which the maximum of $T_\perp$ is obtained. For a two-body decay the reconstructed value is $T_\perp(2) = 1$, and only in the limit of infinite multiplicity does the reconstructed thrust adopt the "theoretical" value $T_\perp(\infty) = 2/\pi \approx 0.64$ for an isotropic production of particles in the transverse plane. Fig. 3 shows the average transverse thrust, $< T_\perp >$, as a function of the E_T of the event. At $E_T = 5$ GeV, $< T_\perp >$ falls with increasing E_T, but changes behaviour for E_T larger than 9 GeV. On the other hand the average multiplicity

of particles in our data is found to increase with increasing E_T. In the absence of a preferred transverse direction, i.e. for an isotropic particle distribution in the transverse plane $< T_\perp >$ is expected to continuously decrease with growing E_T, as a result of the increased average multiplicity. This is demonstrated by the curve in fig. 3 which shows the expectation for thrust in isotropic final states with the same average multiplicity as in the data. The data however does not continue to fall at $E_T > 9$ GeV, contrary to the implications of growing multiplicity. This is an unambiguous signature for an underlying two-body structure in the transverse plane such as a hard scattering process. This evidence is independent of any specific model for soft and hard scattering.

6 Jets in Rapidity Gap Events

To substantiate the above evidence for hard scattering, a search was made for jet structures in the data sample of photoproduction events with a total transverse energy larger than 5 GeV (jet sample), which used an integrated luminosity of 289 nb^{-1}.

A jet finding algorithm was applied to search for jets. The definition of jets was based on transverse energy in the calorimeter contained within cones of radius $R = \sqrt{\Delta\eta^2 + \Delta\varphi^2} = 1.0$ in the space of pseudo-rapidity η and azimuth φ (in radians). For the present study, calorimeter cells from the region $-2 < \eta_{cell} < 2.5$ were considered in the jet search. Within this region, we applied a 'sliding window' with radius $R = 1$ in order to find the cone with the highest transverse energy in the event. The transverse energy E_T within the cone was calculated as a scalar sum of the transverse energy of individual calorimeter cells inside it, while the cone axis is given as the vector pointing from the event vertex to the transverse energy centroid of all cells within the cone [25]. Cones with $E_T > 4$ GeV and pseudo-rapidity in the range $-1 < \eta_{jet} < 1.5$ were accepted as jets in this analysis.

The η_{max} distribution for all γp events of the jet sample containing at least 1 jet is shown in fig. 4. The distribution shows the same characteristics as fig. 1, namely most events have an η_{max} close to η_{Lar}, but a clear signal of events with $\eta_{max} < 2$ is observed. The reduction in the proportion of events in the $\eta_{max} < 1$ region compared to all data (c.f. figure 1) is a consequence of the reduced phase space available for jet production. The η_{max} cut is strongly correlated with M_X, the hadronic mass of the diffractively produced system. Requiring η_{max} to be small preferably selects small M_X events, which have less phase space for the production of jets. The data have been compared with non-diffractive hard scattering γp (PYTHIA; shaded area) and γ-Pomeron (POMPYT; dashed and full lines) predictions. The non-diffractive γp prediction, normalized to the total number of events, cannot account for the η_{max} distribution at smaller values. The POMPYT model, normalized to the number of events with $\eta_{max} < 2$, accounts better for the shape of the η_{max} spectrum, with a slight preference for the configuration including a hard gluon distribution ($G0$) for the Pomeron.

We isolate a diffractive sample by selecting events with $\eta_{max} < 1.5$, as before. Without the requirement for a jet to be present 1632 events are selected. In this rapidity gap sample we find in total 116 events which contain one jet and 19 events which contain 2 jets. From Monte Carlo studies we expect a contamination of 4 non-diffractive γp interactions with at least one jet. The profiles of jets with 4 GeV $< E_{Tjet} <$ 6 GeV and $|\eta_{jet}| < 0.5$ are shown in figure 5 a) and b) and compared with those of jets in photoproduction events selected as above but with the requirement that there be no large forward rapidity gap, namely $\eta_{max} > 1.5$. The profiles are observed to be similar with the exception of the large $\Delta\eta$ region ($1 < \Delta\eta < 2$ in fig. 5 b)). This corresponds to the region required to be devoid of energy in the rapidity gap selection. The diffractive hard scattering Monte Carlo calculation as given by POMPYT describes fairly well the rapidity gap event jet profiles. An example of an event with 2 jets, with an E_{Tjet} of 7

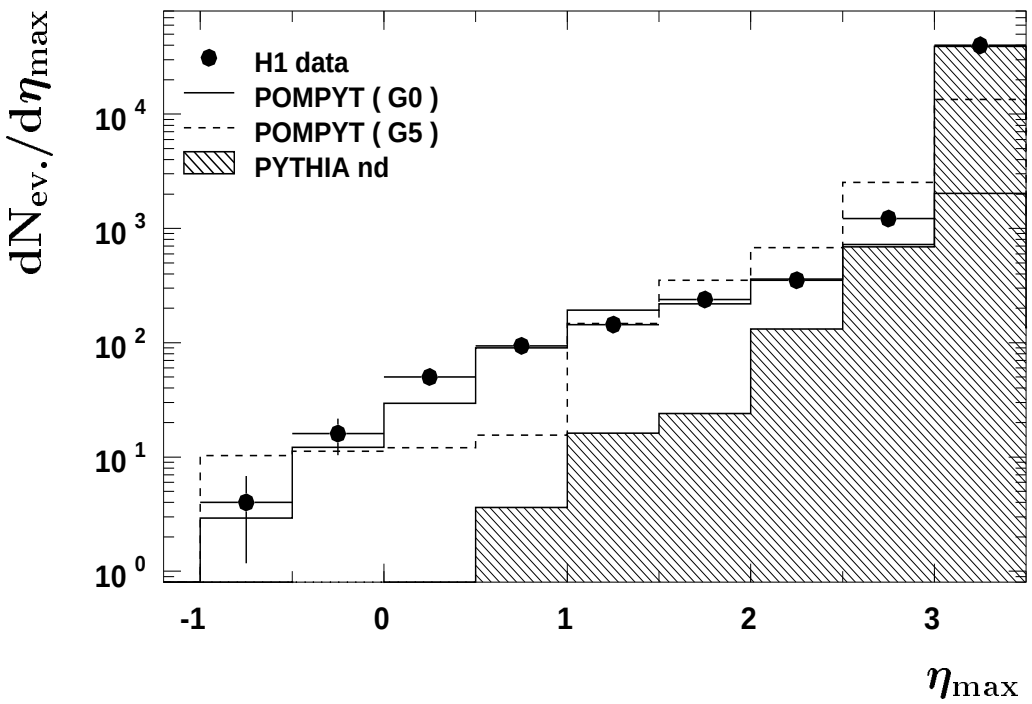

Figure 4: Maximum pseudo-rapidity η_{max} distribution in tagged γp events containing jets with $E_{Tjet} > 4$ GeV in the interval -1.0 $< \eta_{jet} <$ 1.5, compared to Monte Carlo expectations from a non-diffractive process (hatched area) and a diffractive process assuming a Pomeron with hard ($G0$; full line) and soft ($G5$; dashed line) gluon momentum distribution.

GeV and 4 GeV for the jets, is shown in figure 5 c). The back-to-back structure of the 2 jets is clearly observed in the adjacent transverse view of the detector and in the $E(\eta, \varphi)$ distribution.

The transverse energy, E_{Tjet}, spectrum of all jets in the rapidity gap events is shown in figure 6 as well as the distribution of the jet pseudo-rapidities, η_{jet}, and the azimuthal angle between the jets, $\Delta\varphi(jet1 - jet2)$, for the two jet events. For two jet events, the jets are clearly observed to be back-to-back in azimuth, a characteristic feature for a hard scattering process. The E_{Tjet} and the η_{jet} spectra are compared with the shape of the POMPYT expectation, normalized to the number of events with $\eta_{max} < 1.5$, for the hard and soft choices of the Pomeron parton distribution functions. The observed jets behave as expected from parton-parton scattering kinematics and are well described by the POMPYT Monte Carlo predictions. With the present statistics there is no clear preference for one or the other parton distribution, $G0$ or $G5$, in the Pomeron.

With the given selections the relative fractions of 1 and 2 jet events with respect to the total number of events with $E_T > 5$ GeV are 7.1% and 1.2% respectively. To reduce the sensitivity to the $\hat{p}_T^{min}$ cut used in POMPYT and to restrict to a region where the data show dominantly hard scattering features (see fig 3.), a comparison is made of our data with this model by increasing the minimum E_T of the event to 9 GeV. The 1 and 2 jet fractions are then 38.7% and 13.4% respectively, and the ratio (2 jets)/(1 jets) is 0.35 ± 0.09. These results are compared with POMPYT predictions in table 1. The (2 jets)/(1 jets) ratio, which is only weakly sensitive to the remaining soft diffractive contribution, compares favourably with the prediction of a hard Pomeron parton distribution, but it should be noted that this ratio depends somewhat on the choice of the $\hat{p}_T^{min}$ value – changing $\hat{p}_T^{min}$ by 500 MeV leads to a change in the ratio (2 jets)/(1 jets) of 15%.

Thus, the ansatz of hard scattering between partons in the photon and partons in the Pomeron is compatible with the results of the jet analysis of the data.

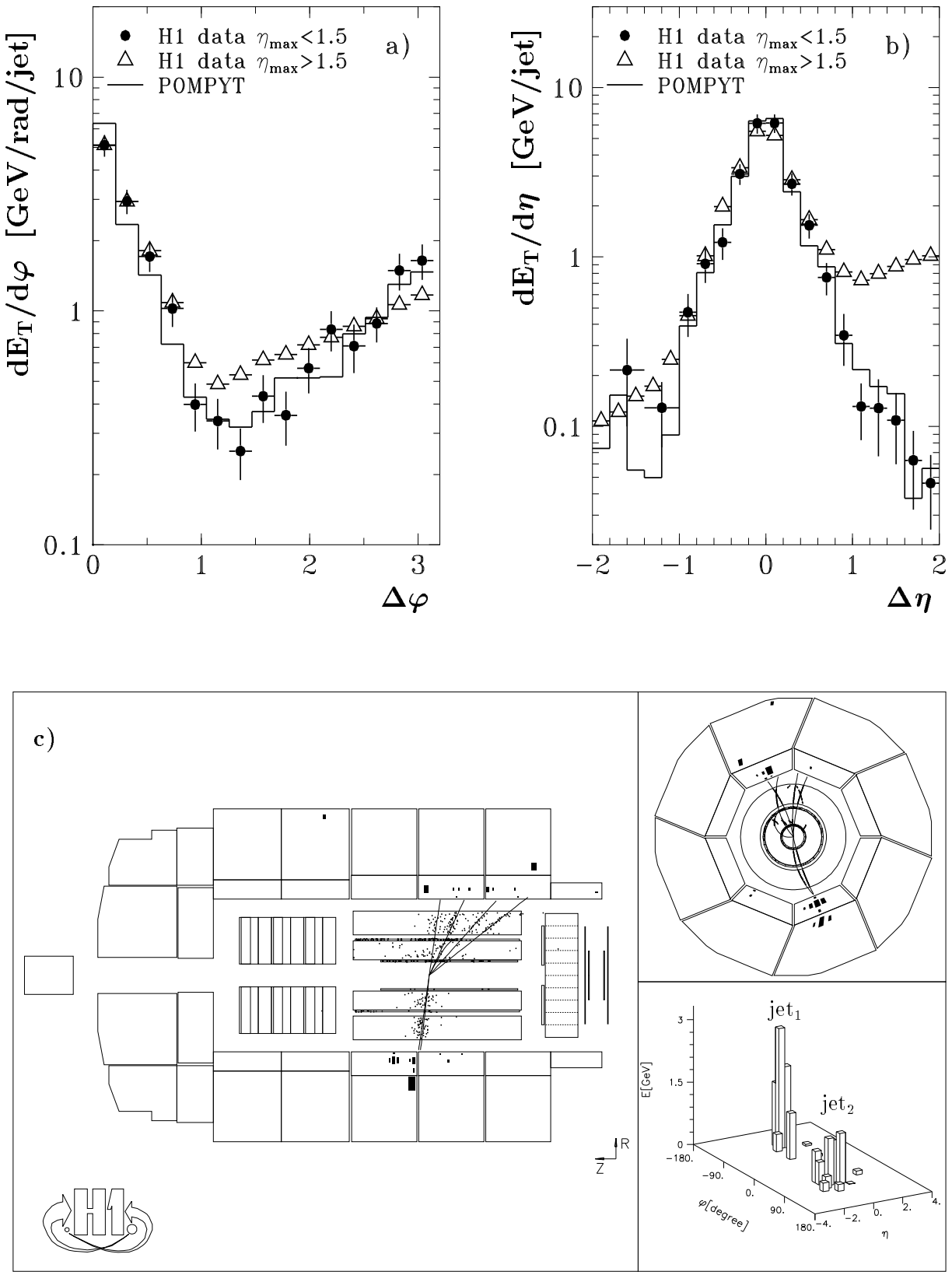

Figure 5: **(a,b)** Transverse energy flow around the jet axis for jets with 4 GeV $< E_{Tjet} <$ 6 GeV and $|\eta_{jet}| < 0.5$: for data with η_{max} <1.5 (circles), for data with η_{max} >1.5 (triangles), and for Monte Carlo events with η_{max} <1.5 (full line). **c)** Two-jet event with a large rapidity gap in the H1 detector.

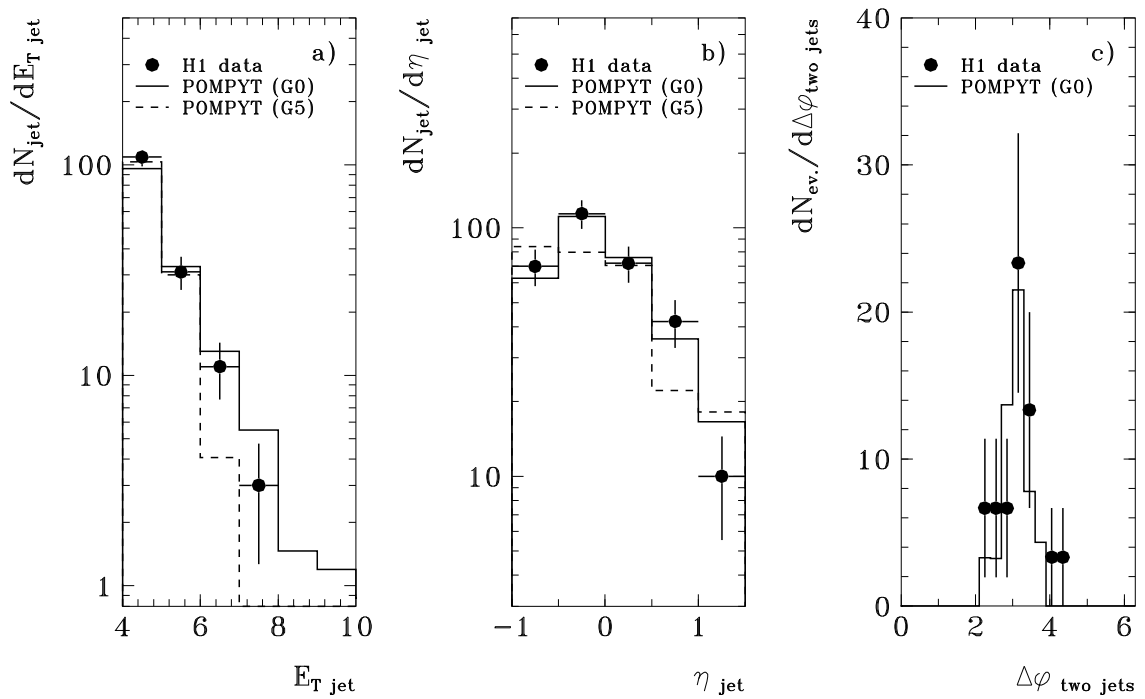

Figure 6: **(a,b)** Inclusive jet distributions for large pseudo-rapidity gap events (η_{max} <1.5): transverse energy E_{Tjet} and pseudo-rapidity η_{jet}. **c)** Distribution of the azimuthal angle $\Delta\varphi$ between the jets for 2 jet events. The data are compared with Monte Carlo predictions assuming a Pomeron with hard ($G0$; full line) and soft ($G5$; dashed line) gluon momentum distribution.

Table 1: Jet rates: data compared to POMPYT Monte Carlo calculations for γp events with $E_T > 9$ GeV and $\eta_{max} < 1.5$, and for jets with $E_{Tjet} > 4$ GeV and $-1 < \eta_{jet} < 1.5$

Sample	1 jet events(%)	2 jet (%)	2-jet/1-jet
Data (142 events)	38.7	13.4	0.35 ± 0.09
POMPYT $G0$ ($\hat{p}_T^{min} = 2$ GeV)	46.4	10.1	0.22 ± 0.05
POMPYT $G5$ ($\hat{p}_T^{min} = 2$ GeV)	27.3	-	< 0.1

7 Conclusions

Events with a large rapidity gap with respect to the proton direction are observed in γp interactions in H1 at HERA. These events are interpreted as diffractive dissociation of the photon. When a sample of such diffractive events is selected by means of a cut $\eta_{max} < 1.5$, features attributable to the presence of hard partonic scattering are observed. The yield of charged tracks from these events, as a function of their transverse momentum, p_T, extends to values which cannot be accounted for in a model of p_T limited phase space, characteristic of our present knowledge of soft diffractive processes. A model which includes hard scattering between partons in the proton and in the Pomeron reproduces well the charged particle yield p_T in the data. The transverse thrust does not decrease with E_T for large transverse energies indicating an underlying two-body structure in the transverse plane, giving a model independ signature for a hard process. Jets are found in the diffractive data sample. In two jet events, the jets are back-to-back in azimuth, substantiating the evidence for hard partonic scattering in diffractive

collisions.

Acknowledgements

We are very grateful to the HERA machine group whose outstanding efforts made this experiment possible. We acknowledge the support of the DESY technical staff. We appreciate the big effort of the engineers and technicians who constructed and maintained the detector. We thank the funding agencies for financial support of this experiment. The non-DESY members of the collaboration also want to thank the DESY directorate for the hospitality extended to them. Finally we would like to thank G. Ingelman for useful discussions.

References

[1] H1 Collab., T. Ahmed *et al.,* Phys. Lett. **B297** (1992) 205

[2] H1 Collab., I. Abt *et al.,* Phys. Lett. **B314** (1993) 436

[3] H1 Collab., I. Abt *et al.,* Phys. Lett. **B328** (1994) 176

[4] ZEUS Collab., M. Derrick *et al.,* Phys. Lett. **B297** (1992) 404

[5] ZEUS Collab., M. Derrick *et al.,* Phys. Lett. **B322** (1994) 287

[6] ZEUS Collab., M. Derrick *et al., Inclusive Jet Differential Cross Sections in Photoproduction at HERA*, DESY preprint DESY 94-176 (1994)

[7] H1 Collab., T. Ahmed *et al.,* Phys. Lett. **B299** (1993) 374;
M. Erdmann *et al., New Results from the H1 Experiment at HERA on Photoproduction, Deep Inelastic Scattering and Searches for New Particles*, DESY preprint DESY 93-077 (1993)
S. Levonian, Proc. of the 28th Rencontre De Moriond, Les Arcs, France, (1993) 529

[8] K. Goulianos, Phys. Rep. **101** (1983) 169

[9] D. Amati *et al.,* Nuovo Cimento **26** (1962) 896

[10] F. E. Low, Phys. Rev. **D12** (1975) 163; S. Nussinov, Phys. Rev. Lett. **34** (1975) 1286

[11] G. Ingelman and P. Schlein, Phys. Lett. **B152** (1985) 256

[12] A. Donnachie and P. V. Landshoff, Phys. Lett. **B191** (1987) 309

[13] N. N. Nikolaev and B. G. Zakharov, Z. Phys. **C53** (1992) 331

[14] UA8 Collab., A. Brandt *et al.,* Phys. Lett. **B297** (1992) 417
UA8 Collab., R. Bonino *et al.,* Phys. Lett. **B211** (1988) 239

[15] H1 Collab., *The H1 detector at HERA*, DESY preprint 93-103 (1993), to be published in Nucl. Instr. and Meth.

[16] H1 Calorimeter Group, B. Andrieu *et al.,* Nucl. Inst. Meth. **A336** (1993) 460

[17] H1 Calorimeter Group, B. Andrieu *et al.,* Nucl. Inst. Meth. **A336** (1993) 499

[18] M. Bengtsson and T. Sjöstrand, Comp. Phys. Commun. **43** (1987) 367;
H.-U. Bengtsson and T. Sjöstrand, Comp. Phys. Commun. **46** (1987) 43;
T. Sjöstrand, CERN-TH-6488-92 (1992)

[19] E612 Collab., T. J. Chapin *et al.,* Phys. Rev. **D31** (1985) 17

[20] P. Bruni and G. Ingelman, Proc. of the Europhysics Conference, Marseilles, France, July 1993, p. 595; DESY preprint DESY 93-187 (1993).

[21] M. Glück, E. Reya and A. Vogt, Z. Phys. **C53** (1992) 127

[22] M. Glück, E. Reya and A. Vogt, Phys. Rev. **D46** (1992) 1973

[23] B. Andersson, G. Gustafson and T. Sjöstrand, Phys. Lett. **B94** (1980) 211;
B. Andersson *et al.,* Phys. Rep. **97** (1983) 31

[24] G. Alberi and G. Goggi, Phys. Rep. **74** (1981) 1

[25] J. E. Huth *et al., Towards a Standardization of Jet Definitions*, Fermilab Conf 90/249-E (1990)